JOURNAL OF Applied Polymer SCIENCE

Special Issue: Sustainable Polymers and Polymer Science Dedicated to the Life and Work of Richard P. Wool

Guest Editors: Dr Joseph F. Stanzione III (Rowan University, U.S.A.)
and Dr John J. La Scala (U.S. Army Research Laboratory, U.S.A.)

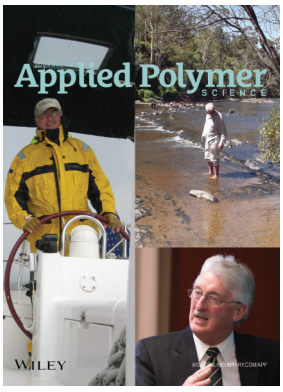

EDITORIAL

REVIEWS

RESEARCH ARTICLES

JOURNAL OF Applied Polymer SCIENCE

Special Issue: Sustainable Polymers and Polymer Science Dedicated to the Life and Work of Richard P. Wool

Guest Editors: Dr Joseph F. Stanzione III (Rowan University, U.S.A.)
and Dr John J. La Scala (U.S. Army Research Laboratory, U.S.A.)

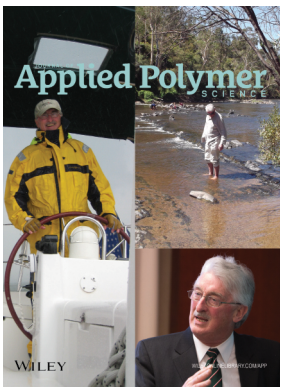

Journal of Applied Polymer Science

Improvement of the mechanical behavior of bioplastic poly(lactic acid)/polyamide blends by reactive compatibilization

Jeongln Gug, Margaret J. Sobkowicz
Department of Plastics Engineering, University of Massachusetts Lowell, Lowell, Massachusetts 01854
Correspondence to: M. J. Sobkowicz (E-mail: Margaret_sobkowiczkline@uml.edu)

ABSTRACT: Polymer blends are of significant interest for reinforcing bioplastics via addition of a second polymer and a blend compatibilizer or in situ reaction. However, increased costs associated with additional materials and extra processing steps can limit the viability of this solution. Here, a simple, continuous reactive extrusion processing method was examined for producing tougher bioplastic blends. *p*-Toluenesulfonic acid (TsOH) catalyst was added to two immiscible biobased polymers, poly(lactic acid) (PLA) and polyamide11 (PA11), to induce ester-amide exchange reaction. The mechanical properties of PLA were improved through mixing with PA11 by introducing copolymers at the interface thereby reducing interfacial tension. The morphology, chemical structure analysis, and tensile testing supported that copolymerization reaction occurred resulting in improved bonding between PLA and PA11 with 0.5 wt % TsOH catalyst in the batch mixing, but depolymerization dominated at higher shear stress (2000 rpm) and catalyst loading (over 2 wt %). The PLA/PA11 blend with 0.5 wt % TsOH catalyst displayed around 50% improvement in elongation at break in twin-screw extruder blending (around 5 min mixing time) at 250 rpm screw speed, which was similar to the improvement using batch mixing (20 min mixing time). © 2016 Wiley Periodicals, Inc. J. Appl. Polym. Sci. **2016**, *133*, 43350.

KEYWORDS: blends; biopolymers & renewable polymers; copolymers; extrusion

Received 6 October 2015; accepted 16 December 2015
DOI: 10.1002/app.43350

INTRODUCTION

Increasing environmental concerns over landfill use, fossil resources and toxic and persistent chemicals demand solutions in the form of more sustainable plastic products. Most plastics are still landfilled after their useful life due to limited recycling options and the complexity of modern plastics products. Polymers from renewable feedstocks offer a solution to the petroleum source problem and often prove to be less toxic than conventional polymers as well. Some bioplastics are also inherently biodegradable, which can be exploited for compostable plastics.[1–5]

Poly(lactic acid) (PLA) is a well-known bio-based and biodegradable thermoplastic polyester with promise for replacing plastic materials based on petroleum resources.[6–10] Importantly, PLA is produced on an industrial scale from corn and sugar beets, and it is becoming cost-competitive with standard packaging, disposable, and medical applications.[11–14] However, PLA has several inferior properties such as low thermal stability, impact resistance and flexibility, as well as limited gas barrier properties.[15–17] Blends with polymers which can compensate for these disadvantages are sought.[18–23]

Polyamide (PA) polymers can be derived from both petroleum and bio-based resources. PAs have high thermal stability, impact and abrasion resistance, chemical resistance and excellent dimensional stability, but are generally more expensive than polyester.[23–28] While many other renewable PAs have been developed recently, PA11 has been produced commercially from castor oil extracts for several decades. To augment PLA with PA11, melt blending is considered an effective and scalable processing method that is greener and less expensive compared with solution blending.

Melt blending is a widely used method to develop new plastic materials with improved property/cost performance and tailor-made properties. The market for polymer blends represents around 40% of the total plastic consumption and this trend is on the rise.[29–32] The selected blend processing technique dictates the dispersion morphology, which in turn determines blend properties.[33–37] From a thermodynamic standpoint, polymer-polymer blends can be miscible, partially miscible or immiscible, however, the last case is the most common in practice due to the entropic penalty of mixing.[38,39]

Several techniques have been explored to improve the compatibility between two immiscible polymers, such as direct addition of a compatibilizer or copolymer, grafting compatible chains via synthetic methods, and using a catalyst to introduce exchange reactions at the interface of polymers producing copolymer in

situ. Introduction of a copolymer with chemical structure from both blend components has the effect of limiting phase separation through reduction in interfacial tension, resulting in smaller domains or even a co-continuous morphology. According to theoretical phase behavior analysis, the morphology is determined by the relationship between viscosity and volume fraction of each component. When two polymers are present in equal volume fractions, the polymer with the lower viscosity forms the continuous phase and the higher viscosity polymer forms dispersed phase of spherical droplets.[40] Previous research investigated blends of PLA and poly(hydroxybutyrate) (PHB),[41,42] starch and PLA,[43,44] chitosan and PLA,[45] PLA and poly(butylene succinate) (PBS),[46–48] PLA and polyamide,[17,49] PLA and polyurethanes,[15] and PLA and polyamide elastomer[19] to improve the mechanical, barrier, recovery, or thermal properties of PLA, but in PLA/PA blend[22,23] low miscibility is still an issue due to incompatibility. Blends of PA11 with polyethylene (PE),[50] polypropylene (PP),[51] or sulfonated polysulfone (SPSF)[52] have demonstrated that compatibilizer or surface modification is required to obtain sufficient phase dispersion in the blends, whereas PA11/PA 6,10[53] resulted in fully miscible blends. *p*-Toluenesulfonic acid (TsOH) was reported to produce significant interchange reaction by creating ester-amide copolymer in the PET/Nylon 6,6 blend,[54,55] Nylon6/PET blend,[56] and PBS/PA6IcoT blend.[57]

Reactive extrusion is widely used for polymer modification because it combines efficient mixing with flexibility of reaction conditions in a continuous process.[58,59] The availability of high speed twin-screw extruders with programmable screw designs has enabled optimized high shear mixing. Combination of forward, neutral, and backward kneading discs maximizes distribution and dispersion in the mixture. The application of high shear stress can also induce more reaction by creating more interfacial area between the phases, resulting in a greater probability of interchange reaction in limited processing time.

In this study, a one-step method for compatibilizing PLA/PA11 blends through catalyzed ester-amide exchange reaction was explored. Two different blending methods were investigated. Batch mixing was explored to study purely kinetic effects at low shear rate, and twin-screw extrusion was used to impart high shear stress for optimal mixing. It was found that both the amount of catalyst and the mixing time control the extent of interchange reaction between ester and amide group in the batch mixing. Higher catalyst loading resulted in significant polymer degradation, as has been observed for PLA blends subjected to high shear.[60] Evidence was found of slightly greater extent of reaction in the extrusion compounding; however, molecular weight degradation superseded improvements to blend properties. This study demonstrates for the first time the effects of ultra-high speed twin-screw extrusion on ester-amide exchange reaction and mechanical properties of polymer blends, in comparison to blends prepared in a low speed batch.

EXPERIMENTAL

Materials

Poly(lactic acid) (PLA) used in this study had a specific gravity of 1.24 g/cm^3, melt flow rate (MFR) of 22 g/10 min (210 °C, 2.16 kg), glass transition temperature (T_g) of 60 °C and melting temperature (T_m) of 166 °C and was produced by NatureWorks LLC (Ingeo™ Biopolymer 3001D). Bio-based Polyamide 11 (PA 11) was supplied by Arkema (Rilsan® BESNO P40 TL) and had a specific gravity of 1.05 g/cm^3, MFR of 3.72 g/10 min (235 °C, 2.16 kg), T_g of 45 °C and T_m of 180 °C. *p*-Toluenesulfonic acid (TsOH, monohydrate, ≥98.5%), and anhydrous ethanol (≥99.5%) were used as purchased from Sigma-Aldrich.

Batch Mixing

PLA and PA11 pellets (total 50 g) were mixed in 50:50 weight ratio at 205 °C for 20 min in a batch mixer (C.W. Brabender® Instruments) with type six sigmoidal rollers at 50 rpm. Both polymers were not dried before mixing. The undried PLA and PA11 pellets were used to increase the possibility of exchange reaction between polymers. It was assumed that undried polymer could be degraded into smaller chains increasing the end groups for more chances for the exchange reaction. PLA was added and melted first followed by addition of PA11. The catalyst (TsOH) with ethanol solvent was added into the mixer at different levels (0.5, 2, 4, and 8 wt % with respect to the total mass of polymer) as soon as PLA and PA11 pellets were melted, as indicated by lower and steady torque readings. The mixed samples were cooled to room temperature and the collected samples were ground into pellets using a laboratory mill (Thomas Wiley® Mill) with a 5 mm sieve.

Twin-Screw Extruder Mixing

PLA and PA11 pellets were ground into powders using a laboratory mill (Thomas Wiley® Milll) with a 3 mm sieve before dry blending. They were then mixed at 50:50 weight ratio using a high intensity blade mixer (Prodex Henschel Mixer). Mixed PLA and PA11 powders were dried over desiccant at 90 °C for 24 h before blending using a laboratory drier machine (RH30, Dri-air industries). The twin-screw compounding extruder (KZW15TW-45/60MG-NH-3000, Technovel Co., Japan) had 15 mm screw diameter with strand die (60:1 *L*/*D*) with a screw program as shown in Figure 1. Extrusion was performed at the following screw speeds: 250, 500, 1000, 2000, and 3000 rpm. The processing temperature was set up to 165 °C for pure PLA, 220 °C for pure PA11 and 205 °C for PLA/PA11 blends except the feed zone was at 190 °C for pure PA11 and PLA/PA11 blends. Vacuum was applied (28 in. Hg) to the vent port just before the die to remove residues and water produced from the condensation reaction. TsOH catalyst solution (0.01 g/mL) in anhydrous ethanol was fed using a peristaltic pump (ISM404B, Ismatec SA, Switzerland) at a flow rate of 2.7 μL/min to introduce 0.5 wt % catalyst on a basis of PLA/PA11 powder feed rate before entering the transition zone of extruder. The blend resin extruded was cooled in a water bath, and then pelletized.

Sample Preparations

For crystalline structure examination, samples were melted on glass slides on a hot plate at 220 °C. For mechanical properties testing, the blend pellets were dried at 90 °C in a vacuum oven for 12 h and then molded into tensile test bars (13 × 3 × 2 mm) using a micro-injection molder (Daca Instruments) at 200 °C. All tensile bars were annealed at 100 °C for 3 h to achieve uniform crystallinity.

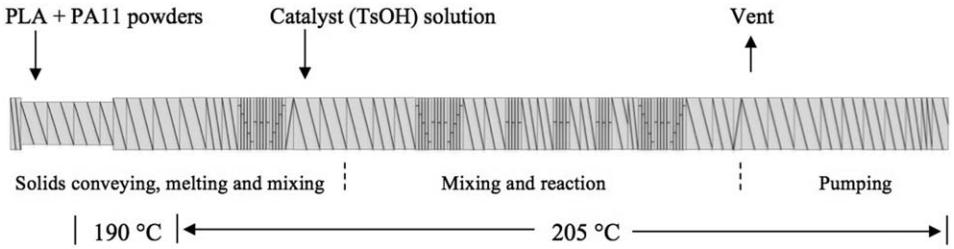

Figure 1. The configuration of the reactive twin-screw extruder for PLA/PA11 blend.

Sample Characterizations

Rheology. The viscosity behavior of neat PLA and PA11 was investigated using a capillary rheometer (LCR 7000, Dynisco) at 205 °C, which is above the melting temperatures of both components (T_m = 180 °C for PA11, 166 °C for PLA). For the viscosity behavior of PLA/PA11 blend, a parallel-plate rheometer (ARES-G2, TA Instruments) equipped with 25 mm diameter stainless steel parallel disks was used. Oscillatory shear measurements were performed with constant strain (within the linear regime) of 10% (PLA/PA11 blends with different catalyst levels from 0.5 to 8 wt %) at 195 °C.

Differential Scanning Calorimetry. The thermal properties of neat PLA, PA11, and PLA/PA11 blends were investigated using differential scanning calorimetry (DSC) (Discovery DSC, TA Instruments). Glass transition temperature (T_g) and melting temperature (T_m) were extracted from the heat flow curves using Trios software (TA Instruments). Samples of 5 mg to 10 mg were sealed in aluminum pans, and the heating and cooling rates were 5 °C/min.

X-ray Diffraction. The X-ray diffraction (XRD) analysis was performed by using a Scintag Inc. XRD Instrument (USA) with Cu-K_α radiation (λ = 0.15406 nm) at room temperature. All samples were annealed at 100 °C for 3 h in the oven before testing. The scanning rate was 2.0°/min and the scanning range was 2 to 40° with a step interval of 0.02°.

Fourier Transform-Infrared Analysis. Fourier transform-infrared (FT-IR) spectroscopy (Nicolet 4700, Thermo Electron Co.) was used to investigate the carbonyl group transition for pure PLA, PA11, and blends of PLA/PA11 with different catalyst loadings. Thin films were melt pressed for each sample, loaded on a diamond attenuated total reflectance crystal and scans were collected over wavenumber range 200 to 3000 cm^{-1}. Depending on the signal to noise ratio, 16 or 40 scans were averaged to get clear peaks.

Nuclear Magnetic Resonance. ^{13}C nuclear magnetic resonance (NMR) spectra of pure PLA, PA11, and blends of PLA/PA11 were obtained on a Bruker Avance DPX 200 spectroscopy with field strength of 200 MHz. For ^{13}C NMR test, solutions of around 25 wt % in *m*-cresol (99%, Alfa Aesar) solvent were prepared.

Tensile Test. The mechanical properties of microinjection molded bars were tested at room temperature using an Instron machine (Model 4444) in accordance with ASTM D638. The tests were conducted at a crosshead speed of 50 mm/min with the strain rate ($\dot{\varepsilon}$) calculated as 3.8/min. At least five samples of each composition were tested.

Field Emission Scanning Electron Microscopy. The state of dispersion of the PLA/PA11 blend was observed by field emission scanning electron microscopy (FE-SEM) (JSM-7401F, Jeol Co., Japan). The blend samples prepared for the tensile test were used. All specimens were cryofractured under liquid nitrogen, and the fracture surfaces were coated with thin layers of gold to aid in imaging. For etching surface investigation, the fractured bars were treated in 0.1*M* sodium hydroxide (NaOH) solution for 24 hr to etch out the PLA phase and then dried another 24 h.

RESULTS AND DISCUSSION

Rheology

The viscosity behavior of pure PLA and PA11 was examined using melt rheology. The capillary rheology result is shown in Figure 2 plotted as corrected viscosity (η_c) *versus* corrected shear rate (γ_c) at 205 °C, i.e., the temperature of blend compounding. The corrected shear viscosity-shear rate relationship was calculated using the Rabinowitch correction method.[61–63] Pure PA11 presents higher viscosity than pure PLA over the observed range of shear rates (1/s) due to stronger hydrogen (H) bonding in amide groups.[64,65]

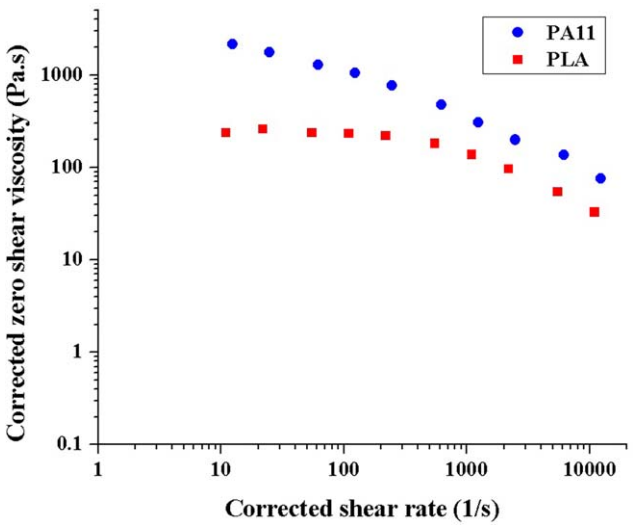

Figure 2. Corrected shear viscosity and shear rate for pure PLA and PA11 unprocessed at 205°C. [Color figure can be viewed in the online issue, which is available at wileyonlinelibrary.com.]

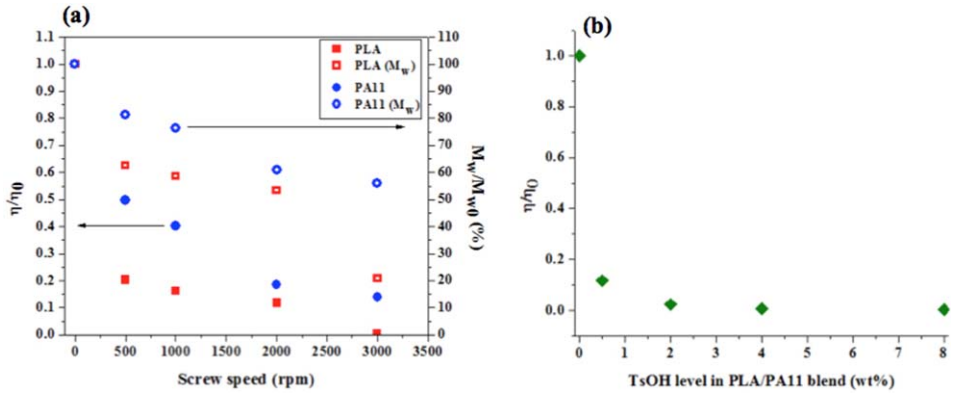

Figure 3. (a) Relative corrected zero shear viscosity (η/η_0) and molecular weight (M_w/M_{w0}) comparison of pure PLA and PA11 at different screw speeds in twin-screw extruder. (b) Relative corrected zero shear viscosity (η/η_0) comparison of PLA/PA11 blend at different TsOH catalyst loads in batch mix. [Color figure can be viewed in the online issue, which is available at wileyonlinelibrary.com.]

The zero shear viscosities of pure PLA, PA11, and PLA/PA11 blend for twin-screw extruder and batch mixing were calculated by fitting the Cross model[66–68] to the viscosity plots, and relative zero shear viscosity (η/η_0) results were converted to relative molecular weight (M_w/M_{w0}) using the Fox-Flory relation for entangled polymer melts.[69] The relative molecular weights for the pure PLA and PA11 are presented in Figure 3. The viscosity of pure PLA decreased around 80%, while that of pure PA11 decreased 50% at 500 rpm screw speed. For the blend of PLA/PA11, increasing catalyst level to 2 wt % resulted in a 90% decrease in relative zero shear viscosity in the batch mix (All blends were tested in using oscillatory shear stress at 195 °C). From the relative molecular weight change it is clear that the polymers are susceptible to degradation due to the high shear stress. It is noted that the extensive degradation was detected by visual inspection with the catalyst present, but the molecular weight of polymers with catalyst added was not measured.

DSC Analysis

Figure 4 shows the second heating trace result of the DSC test for different catalyst loading in PLA/PA11 blend produced by batch mixing. No systematic change was observed in either polymer's glass transition (T_g) using modulated heating ramp, which is widely used to analyze subtle changes in T_g,[70–72] so only the melting point (T_m) variation was examined for PLA/PA11 blends in Table I. When TsOH catalyst is added, the T_m of PLA in the blend presents a split peak indicative of two separate crystal populations, perhaps associated with molecular weight fractions or proximity to the interface. Examination using X-ray diffraction (see Figure 5) does not reveal separate crystal structures, but rather XRD curves display the same peaks as in pure PA11 and PLA. The split melting peaks disappear at higher catalyst level and the melting peak of PA11 is depressed dramatically, shifting from 180 °C to 170 °C at 8 wt %. This reduction in melting temperature is likely due to molecular weight degradation. It is noted that the presence of water and ethanol might affect the depolymerization as well.

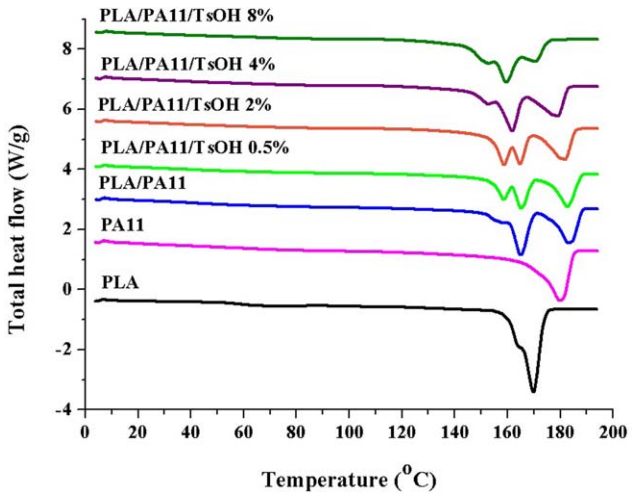

Figure 4. Second heating trace of MDSC for PLA/PA11 blends with different TsOH loadings. [Color figure can be viewed in the online issue, which is available at wileyonlinelibrary.com.]

XRD Analysis

Figure 5 presents the crystalline peaks of the XRD test after annealing blend samples with and without TsOH catalyst. All samples display clear sharp peaks at around 16.5, 19, 20, and 23° of 2θ without shifts in the catalyzed blends. All diffraction patterns are corresponding to the peaks of neat polymers of PLA (16.5 and 19°)[73,74] and PA11 (20 and 23°).[27,75] Although crystallization kinetics were not studied, it does not appear that the dispersed

Table I. Melting Temperature (T_m) for Pure PLA, PA11, and PLA/PA11 Blends

Materials	Blend ratio (wt %)	TsOH level (wt %)	T_m (°C)
PLA	100	—	170
PA11	100	—	180
PLA/PA11	50/50	—	165, 183
PLA/PA11	50/50	0.5	159, 165, 183
PLA/PA11	50/50	2	159, 165, 182
PLA/PA11	50/50	4	153, 162, 179
PLA/PA11	50/50	8	153, 159, 170

Table II. FT-IR Peak Assignment for Pure PLA, PA11, and PLA/PA11 Blends

Materials	Blend ratio (wt %)	TsOH level (wt %)	C=O (ester, PLA) (ppm)	C=O (amide, PA11) (ppm)	N—H (amide, PA11) (ppm)	C—O—C (ester, PLA) (ppm)
PA11	100	—	—	1633	1539	—
PLA	100	—	1747	—	—	1180, 1080
PLA/PA11	50/50	—	1753	1637	1539	1182, 1084
PLA/PA11	50/50	0.5	1751	1635	1541	1182, 1084
PLA/PA11	50/50	2	1755	1635	1541	1182, 1084
PLA/PA11	50/50	4	1755	1635	1543	1182, 1086
PLA/PA11	50/50	8	1755	1635	1539	1180, 1084

PA11 nucleated the PLA because no evidence of altered crystal structure, such as epitaxial crystallization, was observed.[22,57] It should be noted that the total crystallinity of blends did not change in the presence of TsOH catalyst even at higher catalyst level. Summarizing the results of thermal and scattering characterization, two PLA crystal populations emerged with the same structure and without a change in the total amount of crystallinity.

FT-IR Analysis

The normalized FT-IR spectra are shown in Figures 6 and 7, and the peak assignments are given in Table II. No dramatic changes to the spectra were observed for the blends because there was no significant bulk bonding change in produced copolymers. In other words, when ester and amide polymers interchange, ester and amide bonds are formed. However, a depression of the C=O and N—H peaks of PA11 in the blends upon addition of TsOH catalyst was observed rather than a shift of the carbonyl peak location. Normalizing the peak areas to a common marker peak eliminates variation due to different sample thickness, thereby allowing for quantitative comparison.[76] Peak areas were fitted using multi peaks analysis with Gaussian peak type in Origin software, and normalized to the C=O peak of PLA. The PA11 C=O and N—H peak areas decreased significantly when TsOH catalyst was applied. The changes to the PA11 spectrum may indicate a larger extent of interchange reaction occurred when catalyst was added, because the amide bonds appear diluted with respect to ester bonds.[55] No significant difference was observed for higher catalyst level or longer mixing time.

NMR Analysis

To further investigate the chemical structures of copolymer formed in situ, samples were investigated using ^{13}C NMR.[23,57] All possible chemical reaction schemes were drawn according to the literature on ester-amide reactions[30,77,78] using ChemDraw software, and then ^{13}C NMR shift prediction was performed from the copolymer structure drawn. Theoretically, the exchange reaction between polyester (PLA) and polyamide (PA11) can take place through alcoholysis, aminolysis, transesterification and transamidation as shown in Table III. The ChemDraw-simulated chemical shifts were corrected according to the observed C=O signal in *m*-cresol since protic solvents can give rise to weighted average chemical shifts by direct proton transfer.[79,80] The simulated shifts are shown in Table III, and then compared with actual NMR signals in Figure 8. The peak split shown in the C=O region of amide and indicated with arrows was obtained for the catalyzed PLA/PA11 sample in both of batch mixing and twin-screw extrusion. According to the simulated possible

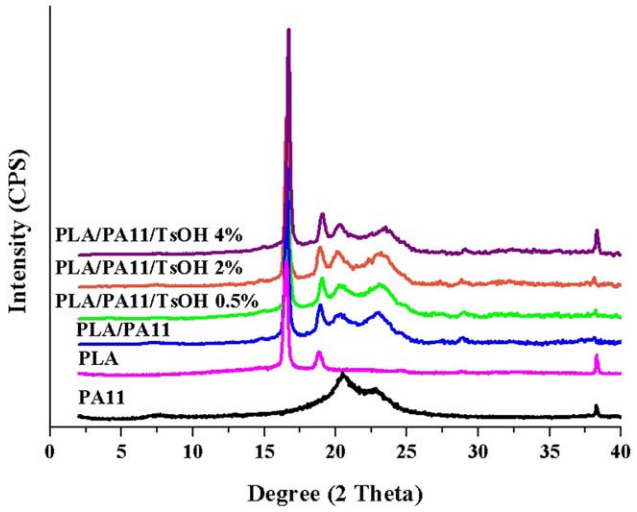

Figure 5. XRD patterns of pure PLA, PA11, and PLA/PA11 blend with different catalyst levels. [Color figure can be viewed in the online issue, which is available at wileyonlinelibrary.com.]

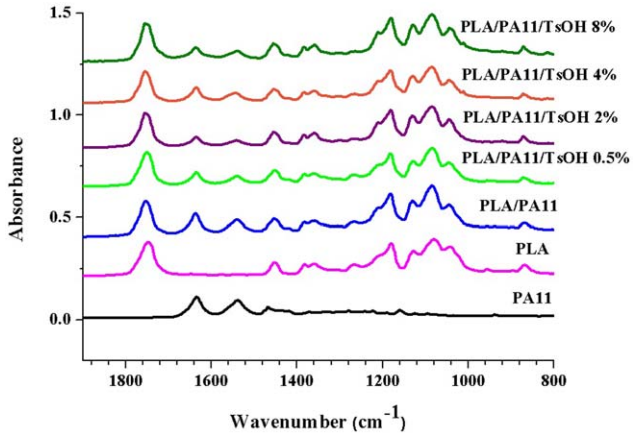

Figure 6. A normalized FT-IR spectrum shows carbonyl group variation for neat polymers and blends (Specific peak information is presented in Table II). [Color figure can be viewed in the online issue, which is available at wileyonlinelibrary.com.]

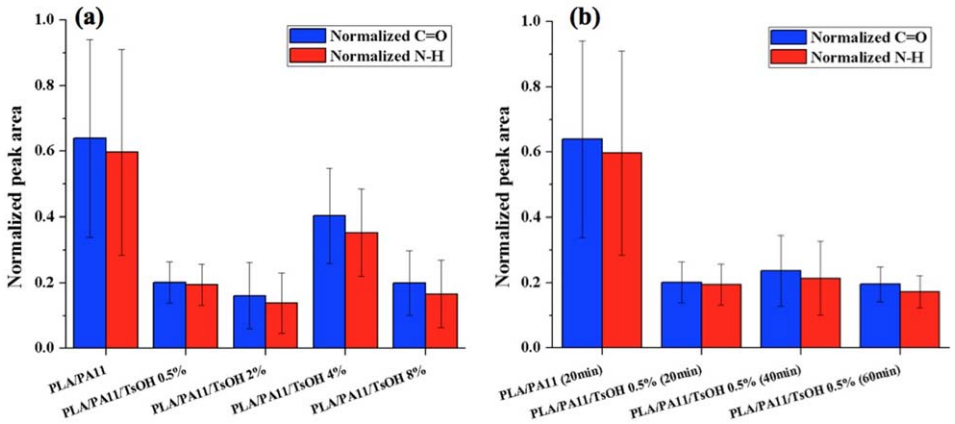

Figure 7. Quantitative peak area of C═O and N─H peak of PA11 based on C═O peak of PLA in blends from normalized FT-IR spectra: (a) different catalyst level; (b) different mixing times (the error bar was obtained from five trials for each specimen. [Color figure can be viewed in the online issue, which is available at wileyonlinelibrary.com.]

products shown in Table III, it appears that aminolysis shown in Figure 9 was the dominant reaction since 181.85 and 181.75 ppm in the simulation model matched to the actual NMR result. Evidence of other reactions such as acidolysis, amide-ester exchange, and alcoholysis was not observed in the NMR spectra. It is noted that the maximum probability of interchange reaction occurs when the ester-amide weight ratio is 50:50.[57]

Mechanical Properties

Figure 10 shows representative stress *versus* strain curves from the tensile testing for the PLA/PA11 blends with and without TsOH in batch and twin-screw extruder mixing. The pure PLA presented brittle behavior without any yielding before fracture, while the PLA/PA11 blend with 0.5 wt % catalyst showed a large improvement in the elongation at break compared with the blend without catalyst. Similar results were obtained for the blend of PLA and PA11 in the extruder mixing, but the PLA/PA11 blend at low screw speed (250 rpm) and excluding catalyst exhibited better elastic behavior compared with batch mixed sample. The addition of 0.5 wt % TsOH enhanced the ductility (elongation at break) of the PLA/PA11 blend over 50%, while the tensile strength was somewhat depressed. The catalyst did

Table III. Simulation of Chemical Shifts in the NMR Spectra of Possible Copolymer Structure

Sequence	Result structures	Carbon	Shift (ppm)
Acidolysis	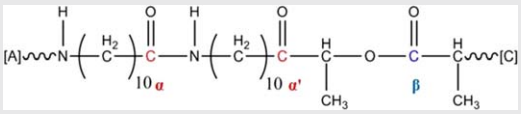	α α′ β	181.76 216.88 175.88
Acidolysis	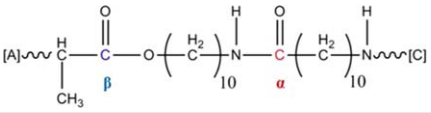	β α	175.88 181.76
Amide-ester exchange	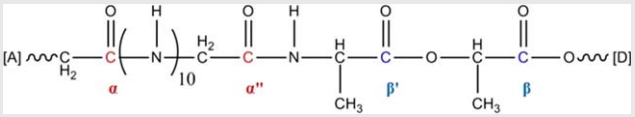	α α″ β′ β	181.76 183.06 176.58 175.88
Amide-ester exchange	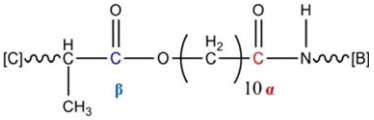	β α	175.88 181.76
Aminolysis	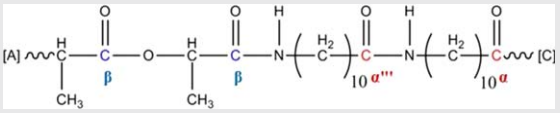	β α‴ α	175.88 181.86 181.76
Alcoholysis	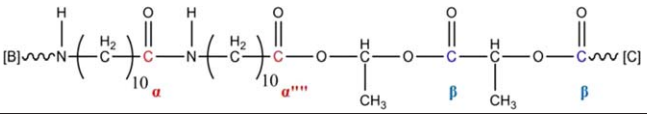	α α⁗ β	181.76 178.18 175.88

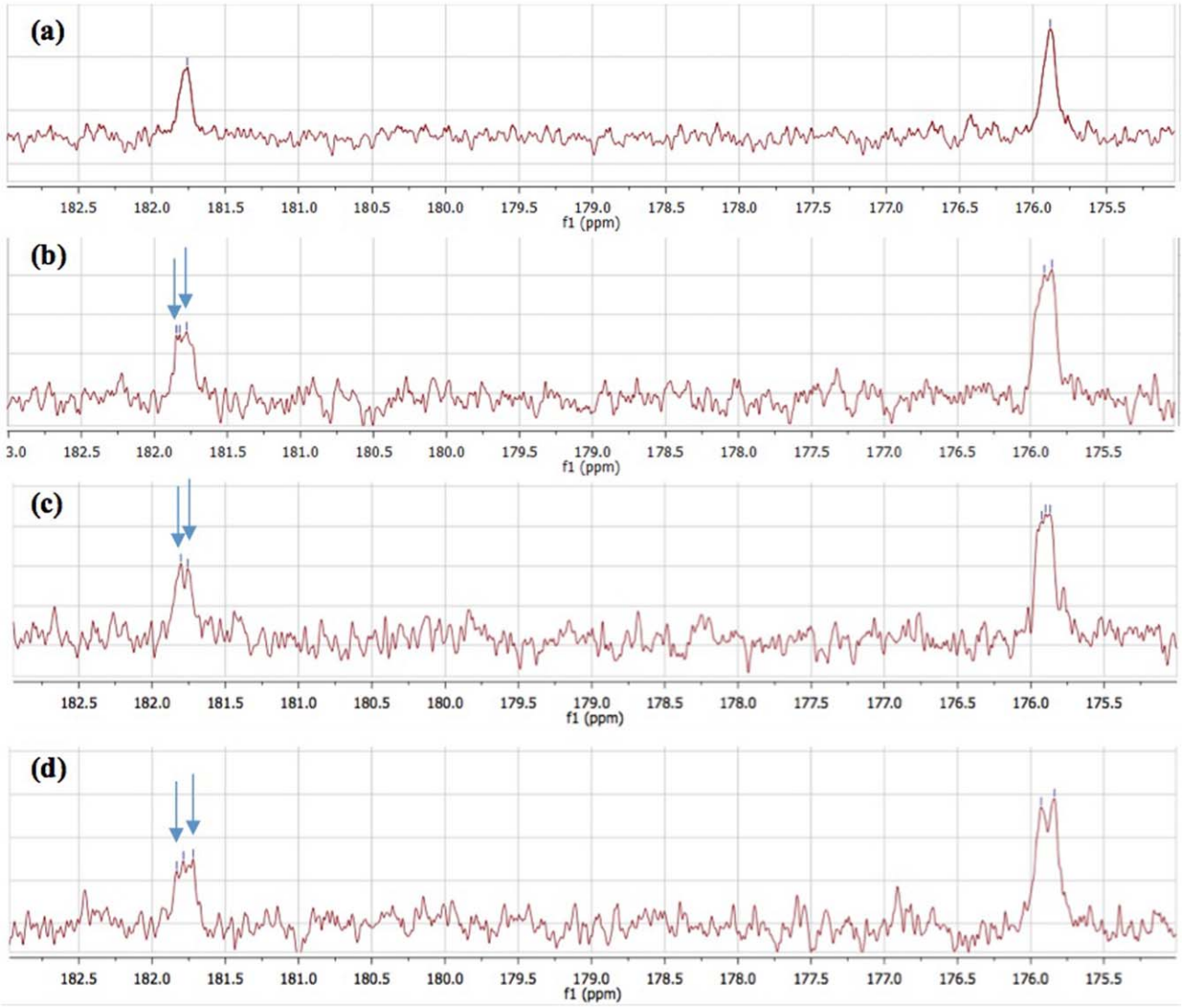

Figure 8. ^{13}C NMR spectra result of PLA/PA11 blends: (a) PLA/PA11 (20 min, batch mix); (b) PLA/PA11/TsOH 0.5% (20 min, batch mix); (c) PLA/PA11/TsOH 0.5% (250 rpm, twin-screw extruder); (d) PLA/PA11/TsOH 0.5% (2000 rpm, twin-screw extruder). [Color figure can be viewed in the online issue, which is available at wileyonlinelibrary.com.]

not positively influence the mechanical properties at higher screw speed (2000 rpm) because the high shear stress resulted in depolymerization that dominated the mechanical behavior. Figure 11 summarizes the results from mechanical testing and clearly shows the benefit of the catalysis at 0.5 wt % as well as the detrimental effects of the highest screw speed. The reason

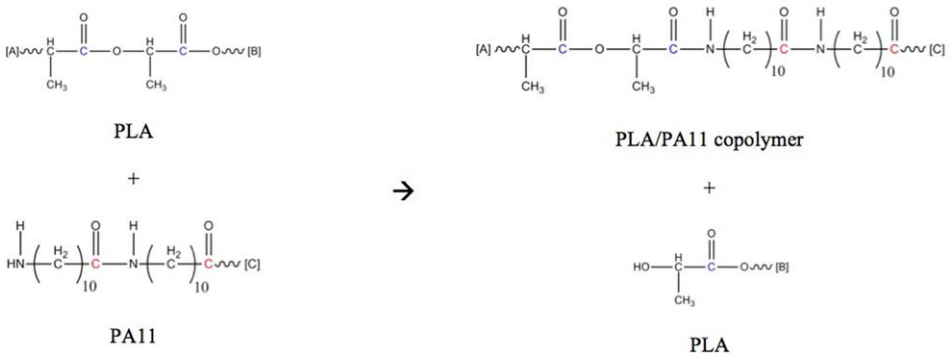

Figure 9. The aminolysis ester-amide exchange reaction formula between PLA and PA11 polymer. [Color figure can be viewed in the online issue, which is available at wileyonlinelibrary.com.]

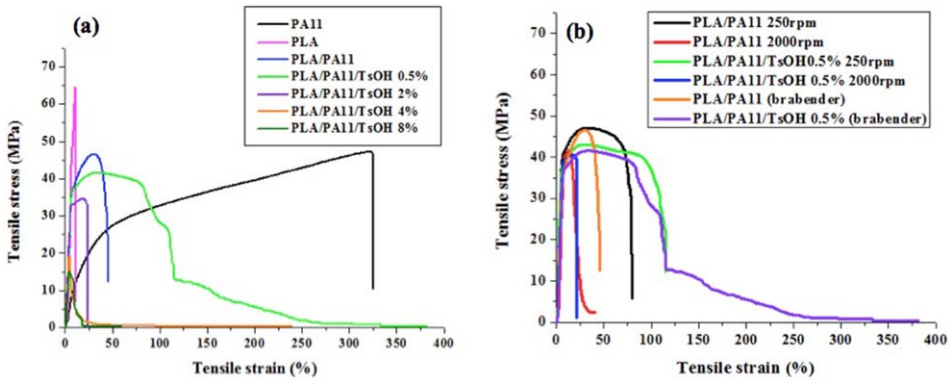

Figure 10. Mechanical test result of (a) the PLA/PA11 blend with different TsOH levels in batch mixing; (b) the PLA/PA11 blend with or without catalyst in different screw speeds of twin-screw extruder. [Color figure can be viewed in the online issue, which is available at wileyonlinelibrary.com.]

for the enhanced elongation and modulus is formation of a new structure bridging the two phases together at the interface. The lowest catalyst weight loading resulted in multi-modal extension, while higher catalyst loading produced brittle failure like pure PLA. These results indicate that a small amount of TsOH catalyst is enough to produce compatibilizing copolymers at the interface, whereas higher levels contribute to depolymerization.

Morphology

Figures 12 to 14 show the morphology change of PLA/PA11 blends prepared by batch or twin-screw extrusion mixing. Figure 12 demonstrates the morphology transition as catalyst level is increased, and clearly shows that PLA and PA11 are immiscible without compatibilizer. Most polymer blends have a two-phase morphology that depends on the relative viscosities and respective volume fraction of the polymers, as shown in eq. (1).[17,22,23] In eq. (1), V indicates the volume fraction and η the zero shear viscosity, where phase 1 is continuous (if $X > 1$), phase 2 is continuous (if $X < 1$) and dual phase continuity exists (for $X \approx 1$). At the 50:50 weight ratio (46:54 volume ratio for PLA and PA11, respectively in this work), the lower viscosity polymer forms the matrix, while the higher viscosity polymer is dispersed because the viscosity ratio is much larger than the volume ratio for the two polymers considered in this work.

$$\frac{V_1}{V_2} \times \frac{\eta_2}{\eta_1} = X \tag{1}$$

Dispersed PA11 droplets exhibit deformed rather than spherical shapes at the 0.5 wt % catalyst loading which may be indicative of the formation of a co-continuous structure due to reduced interfacial tension. The development of a co-continuous structure is also related to the improvement of mechanical properties as shown by the increased elongation at break. This system is similar to that already published about PLA/PA6 blend with 1 wt % compatibilizer[29] and other studies also confirm development of co-continuous morphology after reactive compatibilization.[81] For the catalyst levels above 4 wt %, however, PA11 structures appear to coalesce into larger droplets and the co-continuous phase disappears. Also both maximum tensile stress and elongation at break decreased dramatically as shown Figure 10.

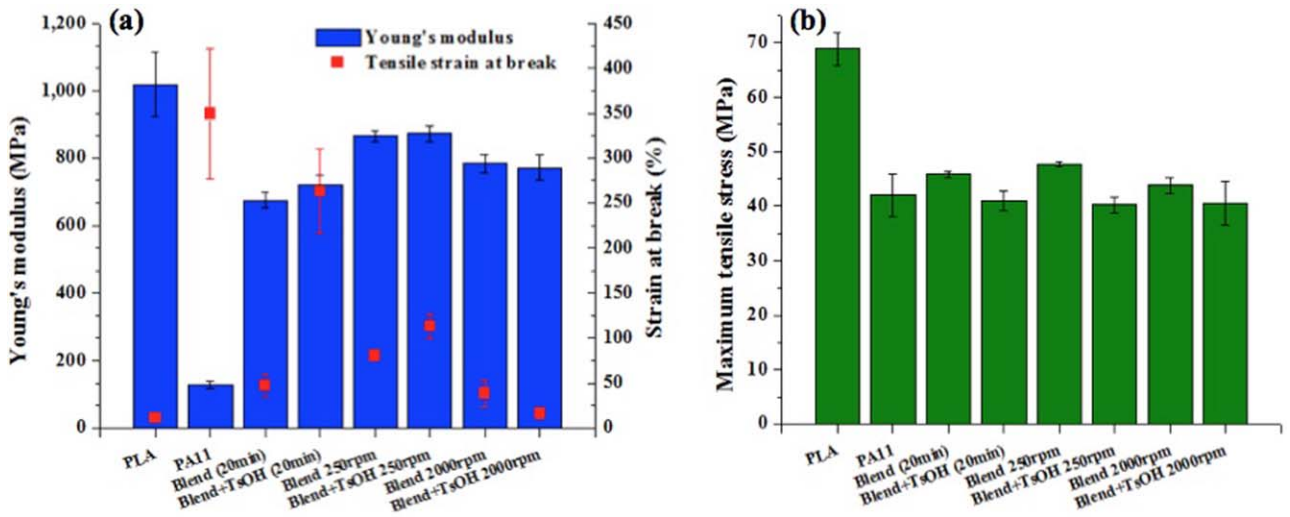

Figure 11. Mechanical properties of the pure polymers and blends (a) Young's modulus (MPa) and tensile strain at break (%), and (b) maximum tensile stress for pure PLA, PA11 and PLA/PA11 blend with or without catalyst (0.5 wt %) in batch mixing and twin-screw extruder (the error bars were calculated from five sample bars for each composition. [Color figure can be viewed in the online issue, which is available at wileyonlinelibrary.com.]

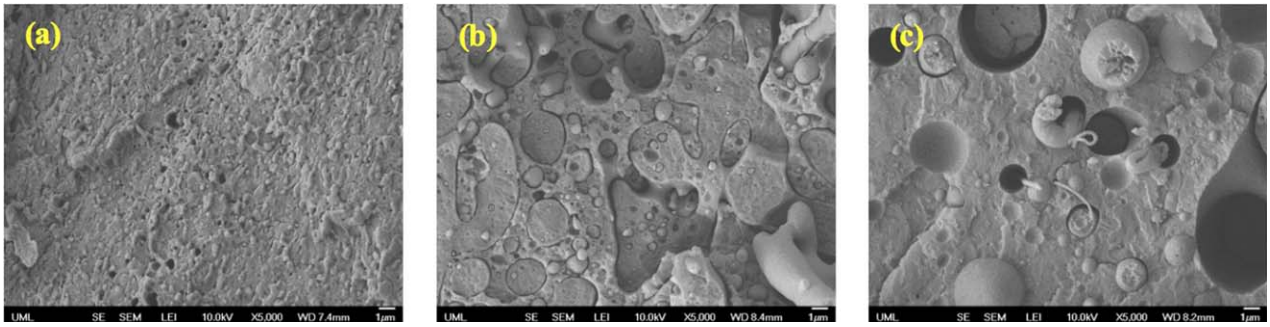

Figure 12. Surface morphology variations of PLA/PA11 batch-blended with different TsOH loadings after tensile testing: (a) PLA/PA11; (b) PLA/PA11/TsOH 0.5%; (c) PLA/PA11/TsOH 8%. [Color figure can be viewed in the online issue, which is available at wileyonlinelibrary.com.]

Figure 13 presents the blend morphology after etching the PLA phase in the blend. This image supports the theory that the continuous phase is composed of PLA, while PA11 is dispersed as droplets. Interestingly, after catalyst addition the PA11 morphology transformed into an elongated continuous structure, which produced better extension in the mechanical test compared with the sample without catalyst. Also lots of small droplets that may be micelles appeared near the droplet boundaries. Previous studies of blend morphology when multiblock and random copolymer compatibilizers are added were consulted in analyzing these results.[82] When a multiblock copolymer is well defined at the interface, the interfacial tension and domain size

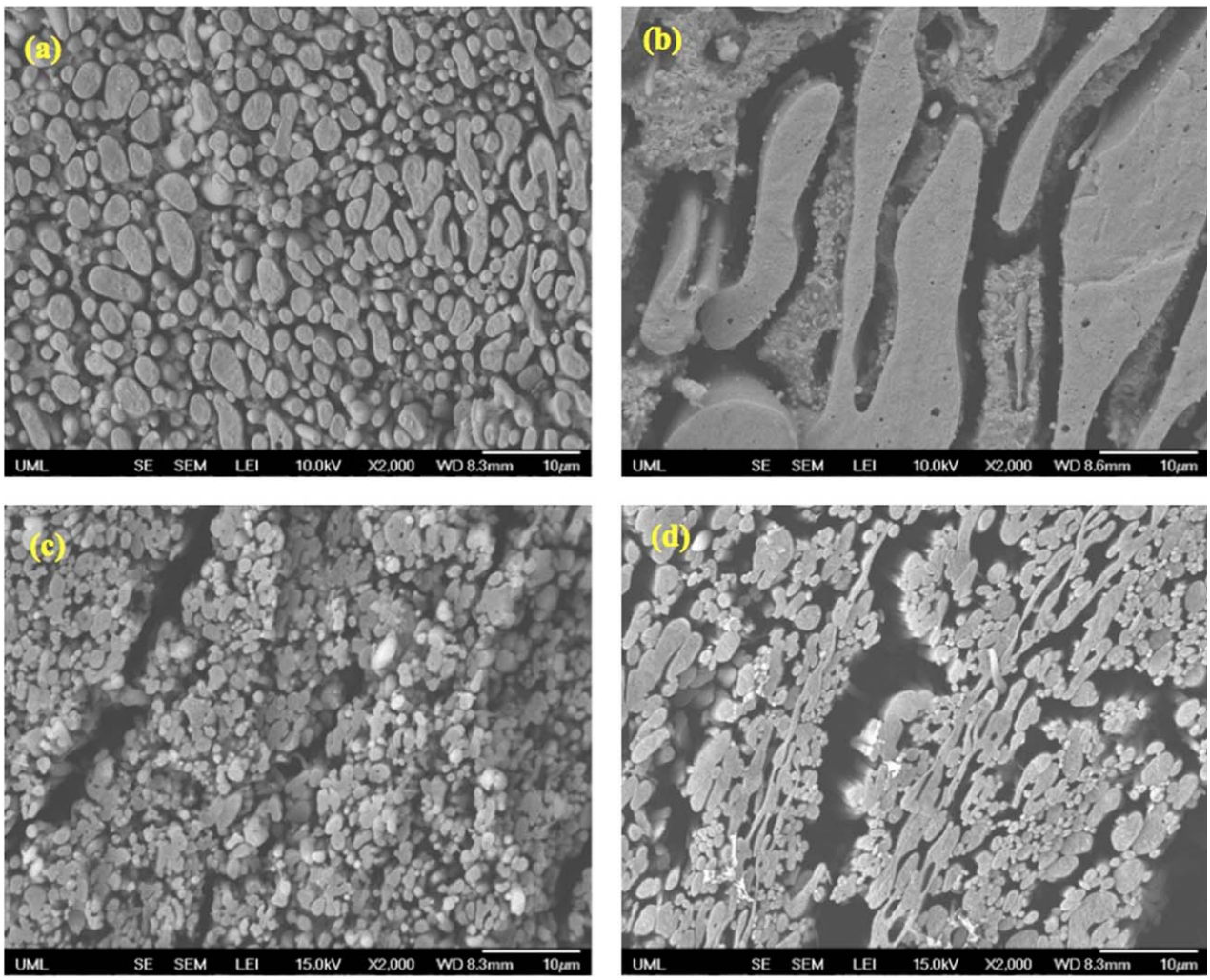

Figure 13. Surface morphology transition of PLA/PA11 blend after etching out PLA phase in the blend: (a) PLA/PA11 (batch mix); (b) PLA/PA11/TsOH 0.5% (batch mix); (c) PLA/PA11 (250 rpm, twin-screw extruder); (d) PLA/PA11/TsOH 0.5% (250 rpm, twin-screw extruder). [Color figure can be viewed in the online issue, which is available at wileyonlinelibrary.com.]

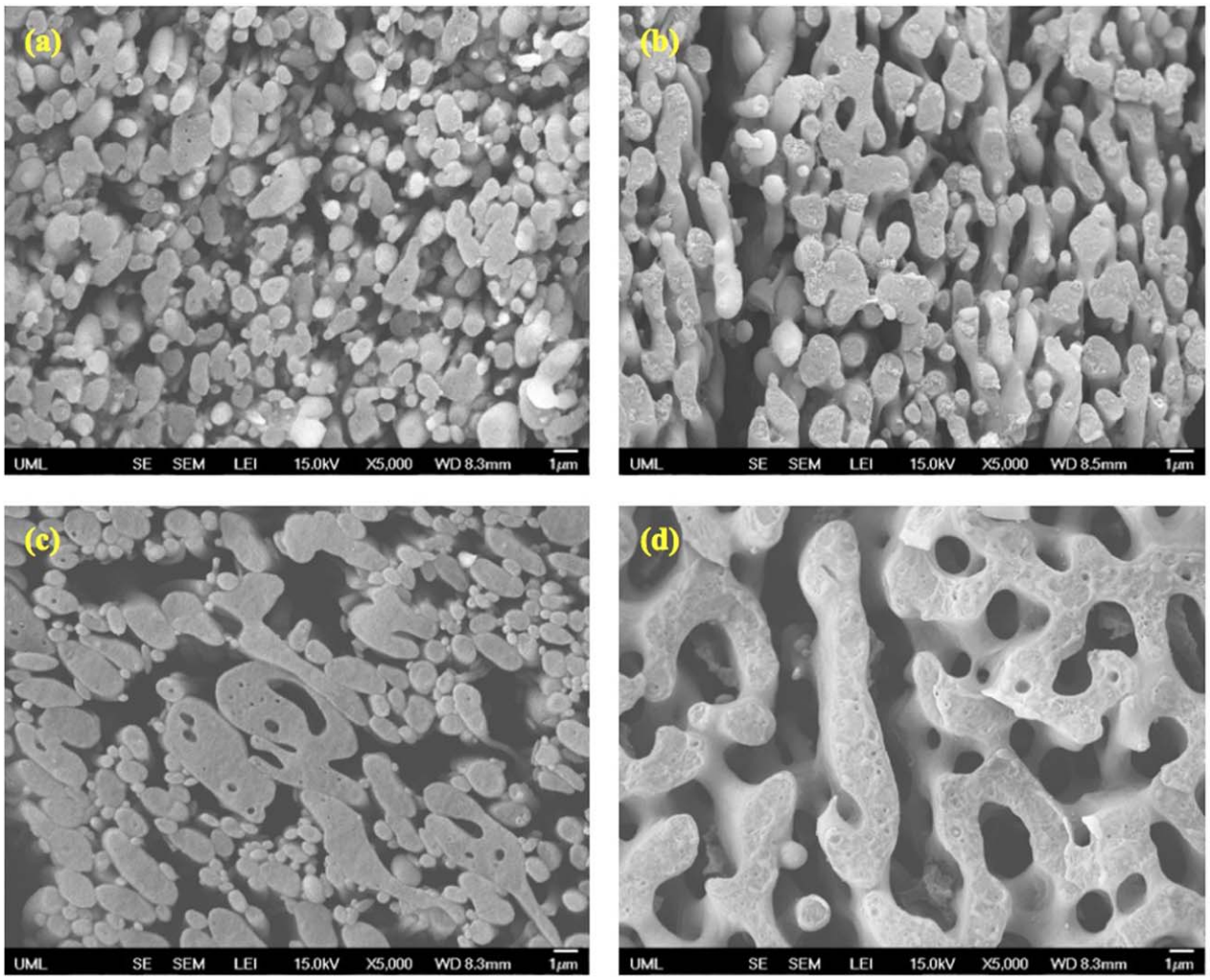

Figure 14. Surface morphology transition of PLA/PA11 blends with and without catalyst at different screw speeds after etching out PLA phase in the blend: (a) PLA/PA11 at 250 rpm; (b) PLA/PA11 at 2000 rpm; (c) PLA/PA11/TsOH 0.5% at 250 rpm; (d) PLA/PA11/TsOH 0.5% at 2000 rpm. [Color figure can be viewed in the online issue, which is available at wileyonlinelibrary.com.]

decrease but interfacial thickness increases. In contrast, random copolymers are unable to localize at the interface, so rather disperse in either homopolymer phase. Catalyst loading over 4 wt % may accelerate chain scission, creating larger droplets as well as disappearance of the co-continuous structure. This morphology transition could be linked to the mechanical properties in that the co-continuous structure increases ductility, while larger aggregated droplets reduce the ductility.

Extruded PLA/PA11 blends exhibited similar results to the blends prepared by batch mixing. Extrusion reduced the droplet size due to high shear, and the blend without catalyst produced more aggregated particles, which could explain the better mechanical behavior compared with the blend without catalyst produced in the batch mixer. A random continuous morphology developed upon addition of catalyst. The morphology change was not as dramatic for the extruded blends as for the batch mixed blends. Nevertheless, extruded blends with catalyst did show improved mechanical properties including higher Young's modulus and strain at break.

The morphology of PLA/PA11 blend processed by twin-screw extrusion in Figure 14 shows that a larger length scale phase structure was produced at higher screw speed, likely due to the reduced molecular weight and increased probability of coalescence. As in the PLA/PA11 sample prepared by batch mixer, it was found that 0.5 wt % TsOH catalyst influenced the morphology, producing more deformed droplets at 250 rpm, while the same catalyst level increased the extent of interconnection at the higher screw speed of 2000 rpm. The higher screw speed samples were brittle as well due to reduced molecular weight, as in the higher catalyst levels in the batch blending experiments. This result was expected because the higher shear stress likely degraded the molecular weight, as confirmed by the rheology results presented before earlier.

CONCLUSIONS

PLA and PA11 polymer were melt blended at equal weight fraction using two different processes: batch and twin-screw extruder mixing, both with and without TsOH as a catalyst.

The bioplastic based on PLA matrix was successfully compatibilized through interchange reaction in both processes improving the elastic behavior remarkably. TsOH proved to be an effective catalyst for the ester-amide exchange reaction, as observed through morphology, mechanical properties and NMR spectra investigation. Co-continuous morphology was observed for the catalyzed blends. Copolymers served as compatibilizers and reduced the interfacial tension between the two phases. As a result, the blend with 0.5 wt % catalyst showed dramatically improved mechanical properties including around 50% increase in elongation at break. There was no significant change in the crystalline structure or overall crystallinity. High catalyst level (over 2 wt %) and shear stress (higher than 2000 rpm) should be avoided to prevent degradation and deterioration of the blend properties. This reactive extrusion work has the potential to reduce the processing time and complexity, and result in superior blend properties.

ACKNOWLEDGMENTS

The authors acknowledge the funding from the National Science Foundation (NSF) (CMMI—1350445). The authors are also thankful to Professor Robert Malloy and Azadeh Farahanchi for their help with the high speed extrusion.

REFERENCES

1. Gross, R. A. *Science* **2002**, *297*, 803.
2. Yu, L.; Dean, K.; Li, L. *Prog. Polym. Sci.* **2006**, *31*, 576.
3. Gandini, A. *Macromolecules* **2008**, *41*, 9491.
4. Tschan, M. J. L.; Brulé, E.; Haquette, P.; Thomas, C. M. *Polym. Chem.* **2012**, *3*, 836.
5. Garlotta, D. *J. Polym. Environ.* **2001**, *9*, 63.
6. Ljungberg, N.; Wesslén, B. *Polymer* **2003**, *44*, 7679.
7. Ljungberg, N.; Wesslén, B. *Biomacromolecules* **2005**, *6*, 1789.
8. Madhavan Nampoothiri, K.; Nair, N. R.; John, R. P. *Bioresour. Technol.* **2010**, *101*, 8493.
9. Jonoobi, M.; Harun, J.; Mathew, A. P.; Oksman, K. *Compos. Sci. Technol.* **2010**, *70*, 1742.
10. Baghaei, B.; Skrifvars, M.; Rissanen, M.; Ramamoorthy, S. K. *J. Appl. Polym. Sci.* **2014**, *131*, DOI: 10.1002/app.40534.
11. Henton, D. E.; Gruber, P.; Lunt, J.; Randall, J. *Nat. Fibers Biopolym.* **2005**, 527.
12. Williams, D. F. *J. Mater. Sci.* **1982**, *17*, 1233.
13. Emil, S. E.; Albert, P. R. U.S. Pat. 3,297,033, January 10, **1967**.
14. Shen, L.; Worrell, E.; Patel, M. *Biofuels Bioprod. Biorefining* **2010**, *4*, 25.
15. Li, Y.; Shimizu, H. *Macromol. Biosci.* **2007**, *7*, 921.
16. Rasal, R. M.; Janorkar, A. V.; Hirt, D. E. *Prog. Polym. Sci.* **2010**, *35*, 338.
17. Nuzzo, A.; Coiai, S.; Carroccio, S. C.; Dintcheva, N. T.; Gambarotti, C.; Filippone, G. *Macromol. Mater. Eng.* **2014**, *299*, 31.
18. Carlson, D.; Nie, L.; Narayan, R.; Dubois, P. *J. Appl. Polym. Sci.* **1999**, *72*, 477.
19. Zhang, W.; Chen, L.; Zhang, Y. *Polymer* **2009**, *50*, 1311.
20. Feng, F.; Ye, L. *J. Macromol. Sci. Phys.* **2010**, *49*, 1117.
21. Inkinen, S.; Hakkarainen, M.; Albertsson, A. C.; Södergård, A. *Biomacromolecules* **2011**, *12*, 523.
22. Stoclet, G.; Seguela, R.; Lefebvre, J. M. *Polymer* **2011**, *52*, 1417.
23. Patel, R.; Ruehle, D. A.; Dorgan, J. R.; Halley, P.; Martin, D. *Polym. Eng. Sci.* **2013**, *54*, 1523.
24. Jacques, B.; Werth, M.; Merdas, I.; Thominette, F.; Verdu, J. *Polymer* **2002**, *43*, 6439.
25. Wang, B.; Hu, G.; Zhao, X.; Gao, F. *Mater. Lett.* **2006**, *60*, 2715.
26. Fornes, T. D.; Paul, D. R. *Macromolecules* **2004**, *37*, 7698.
27. Zhang, Q.; Mo, Z.; Zhang, H.; Liu, S.; Cheng, S. Z. D. *Polymer* **2001**, *42*, 5543.
28. Zhang, X.; Xie, T.; Yang, G. *Polymer* **2006**, *47*, 2116.
29. Kucharczyk, P.; Sedlarik, V.; Miskolczi, N.; Szakacs, H.; Kitano, T. *J. Reinf. Plast. Compos.* **2012**, *31*, 189.
30. Koning, C.; Van Duin, M.; Pagnoulle, C.; Jerome, R. *Prog. Polym. Sci.* **1998**, *23*, 707.
31. Paul, D. R. Polymer Blends; Elsevier: NY, **1978**; Vol. *2*, Chapter 1, p 2.
32. Shonaike, G. O.; Simon, G. P. Polymer Blends and Alloys; CRC Press: NY, **1999**; Vol. *52*, Chapter 1, p 1.
33. Willemse, R. C. *Polymer.* **1999**, *40*, 2175.
34. Ryan, A. *J. Nat. Mater.* **2002**, *1*, 8.
35. Ajji, A.; Utracki, L. A. *Polym. Eng. Sci.* **1996**, *36*, 1574.
36. Asadinezhad, A.; Yavari, A.; Jafari, S. H.; Khonakdar, H. A.; Böhme, F.; Hässler, R. *Polym. Bull.* **2005**, *54*, 205.
37. Scott, C. E.; Macosko, C. W. *Polymer.* **1995**, *36*, 461.
38. Utracki, L. A. Commercial Polymer Blends; Kluwer Academic Publishers: Netherlands, **1998**; Vol. *1*, Chapter 2, pp 83–86.
39. Utracki, L. A. Polymer Blends Handbook; Kluwer Academic Publishers: Netherlands: **2002**; Vol. *1*, Chapter 2, p 123.
40. Sperling, L. H. Introduction to Physical Polymer Science; Wiley: NJ, **2005**; Vol. *4*, Chapter 13, p 706.
41. Ohkoshi, I.; Abe, H.; Doi, Y. *Polymer* **2000**, *41*, 5985.
42. Koyama, N.; Doi, Y. *Polymer* **1997**, *38*, 1589.
43. Ke, T.; Sun, X. *J. Appl. Polym. Sci.* **2001**, *81*, 3069.
44. Park, J. W.; Im, S. S.; Kim, S. H.; Kim, Y. H. *Polym. Eng. Sci.* **2000**, *40*, 2539.
45. Suyatma, N. E.; Copinet, A.; Tighzert, L.; Coma, V. *J Polym. Environ.* **2004**, *12*, 1–6.
46. Wang, R.; Wang, S.; Zhang, Y.; Wan, C.; Ma, P. *Polym. Eng. Sci.* **2009**, *49*, 26.
47. Homklin, R.; Hongsriphan, N. *Energy Procedia* **2013**, *34*, 871.
48. Zhou, J.; Yao, Z.; Zhou, C.; Wei, D.; Li, S. *J. Appl. Polym. Sci.* **2014**, DOI: 10.1002/app.40773.
49. Rashmi, B. *J. Express Polym. Lett.* **2015**, *9*, 721.

50. Hu, G.; Wang, B.; Zhou, X. *Mater. Lett.* **2004**, *58*, 3457.
51. Liang, Z.; Williams, H. L. *J. Appl. Polym. Sci.* **1992**, *44*, 699.
52. Deimede, V.; Fragou, K.; Koulouri, E.; Kallitsis, J.; Voyiatzis, G. *Polymer* **2000**, *41*, 9095.
53. Ruehle, D. A.; Perbix, C.; Castañeda, M.; Dorgan, J. R.; Mittal, V.; Halley, P.; Martin, D. *Polymer* **2013**, *54*, 6961.
54. Pillon, L. Z.; Utracki, L. A. *Polym. Eng. Sci.* **1984**, *24*, 1300.
55. Pillon, L. Z.; Utracki, L. A.; Pillon, D. W. *Polym. Eng. Sci.* **1987**, *27*, 562.
56. Samperi, F.; Puglisi, C.; Alicata, R.; Montando, G. *J. Polym. Sci. Part A: Polym. Chem.* **2003**, *41*, 2778.
57. Yao, Z.; Sun, J.; Wang, Q.; Cao, K. *Ind. Eng. Chem. Res.* **2011**, *51*, 751.
58. Raquez, J. M.; Degée, P.; Nabar, Y.; Narayan, R.; Dubois, P. *Comptes Rendus Chim.* **2006**, *9*, 1370.
59. Vergnes, B.; Berzin, F. *Comptes Rendus Chim.* **2006**, *9*, 1409.
60. Spinella, S.; Cai, J.; Samuel, C.; Zhu, J.; McCallum, S. A.; Habibi, Y.; Raquez, J. M.; Dubois, P.; Gross, R. A. *Biomacromolecules* **2015**, *16*, 1818.
61. Sinthavathavorn, W.; Nithitanakul, M.; Grady, B. P.; Magaraphan, R. *Polym. Bull.* **2009**, *63*, 23.
62. Hamad, K.; Kaseem, M.; Deri, F. *Polym. Bull.* **2010**, *65*, 509.
63. Chien, R. D.; Jong, W. R.; Chen, S. C. *J. Micromech. Microeng.* **2005**, *15*, 1389.
64. Coleman, M. M.; Skrovanek, D. J.; Hu, J.; Painter, P. C. *Macromolecules* **1988**, *21*, 59.
65. Skrovanek, D. J.; Painter, P. C.; Coleman, M. M. *Macromolecules* **1986**, *19*, 699.
66. Hameed, T.; Hussein, I. A. *Polymer* **2002**, *43*, 6911.
67. Khor, C. Y.; Ariff, Z. M.; Ani, F. C.; Mujeebu, M. A.; Abdullah, M. K.; Abdullah, M. Z.; Joseph, M. A. *Int. Commun. Heat Mass Transf.* **2010**, *37*, 131.
68. Silva, A. L. N.; Rocha, M. C.; Coutinho, F. M. *Polym. Test.* **2002**, *21*, 289.
69. Fox, T. G.; Flory, P. J. *J. Phys. Chem.* **1951**, *55*, 221.
70. Wang, Y.; Goh, S. H.; Chung, T. S. *Polymer* **2007**, *48*, 2901.
71. Zhao, J.; Ediger, M. D.; Sun, Y.; Yu, L. *Macromolecules* **2009**, *42*, 6777.
72. Song, M.; Hourston, D. J.; Pollock, H. M.; Hammiche, A. *Polymer* **1999**, *40*, 4763.
73. Zhong, W.; Ge, J.; Gu, Z.; Li, W.; Chen, X.; Zang, Y.; Yang, Y. *J. Appl. Polym. Sci.* **1999**, *74*, 2546.
74. Fukushima, K.; Kimura, Y. *Polym. Int.* **2006**, *55*, 626.
75. Liu, T.; Ping Lim, K.; Chauhari Tjiu, W.; Pramoda, K. P.; Chen, Z. K. *Polymer* **2003**, *44*, 3529.
76. Kolhe, P.; Kannan, R. M. *Biomacromolecules* **2003**, *4*, 173.
77. Fakirov, S. Transreactions in Condensation Polymers; Wiley: NY, **1999**; Chapter 10, p 411.
78. Kotliar, A. M. *J. Polym. Sci. Macromol. Rev.* **1981**, *16*, 367.
79. Maciel, G. E.; Ruben, G. C. *J. Am. Chem. Soc.* **1963**, *85*, 3903.
80. Maciel, G. E.; Natterstad, J. J. *J. Chem. Phys.* **1965**, *42*, 2752.
81. Tol, R. T.; Groeninckx, G.; Vinckier, I.; Moldenaers, P.; Mewis, J. *Polymer* **2004**, *45*, 2587.
82. Joseph, S.; Lauprêtre, F.; Negrell, C.; Thomas, S. *Polymer* **2005**, *46*, 9385.